Article

Operation Problems of Solar Panel Caused by the Surface Contamination

Dávid Matusz-Kalász * and István Bodnár

Institute of Physics and Electrical Engineering, University of Miskolc, 3515 Miskolc-Egyetemváros, Hungary; vegybod@uni-miskolc.hu
* Correspondence: elkmkd@uni-miskolc.hu

Abstract: Solar panels have been widely criticized for their weather dependence and slowly improving efficiency. Several external factors can further increase the efficiency of solar panels, e.g., shading effect and surface contamination. We investigated the warming effect and the negative impact of these factors on energy production during the research. The continuous operation at high temperatures can modify the crystal structure of solar cells in these hot spots. The electroluminescence (EL) images and thermal imaging measurements show crystal structure failure. In addition to structural damage and rapid aging of the solar cells, contaminants can cause power losses of up to 10%.

Keywords: solar panel; experimental investigation; dust concentration; power loss; temperature increase

1. Introduction

In the last few decades, the World's energy demand has grown approximately five-fold, attributed to population growth and the industry of developing countries (and for many other reasons). The efficiency of energy production and consumption must also be increased to avoid excessive demand for our energy. Solar panels produce direct current and direct voltage, which give the electrical power of a solar cell that produces these parameters. Manufacturers and distributors typically characterize their products with peak performance. However, the solar cells very rarely reach this peak value. Environmental effects influence the lifetime of the solar panel. Solar radiation and the ambient temperature have an important role because these effects increase the surface temperature of the solar panels, causing a decrease in power. The deposited dust and its shadow effect further degrade the performance. The effect of the surface contamination of a photovoltaic panel on its electrical parameters is presented in this paper [1]. In addition, the fundamental goal of this research is to establish a correlation between the surface contamination and the electrical or structural defects of the photovoltaic panel (electroluminescence test).

During the operation of solar power plants, dust deposited on the solar cell surface is an increasing problem. In addition to reducing the energy production of the solar panel, the deposited dust causes more heating. If the solar panel operates at permanently high temperatures, it will be damaged. In an industrial environment, this phenomenon is becoming more pronounced. The amount of dust deposited on the panel during operation cannot be determined accurately. However, the electrical parameters and the solar panel temperature (temperature distribution) can be quickly and accurately measured. Therefore, laboratory tests were needed to show the influencing effect of different amounts of contaminants. Based on the measured electrotechnical parameters, the results obtained during the tests can conclude how to operate an outside solar panel if it is dusty.

Regardless of the maximum efficiency of the manufacturing technology and the purity of the used materials, external factors (e.g., polluted surface, load levels, and high temperature) can reduce the efficiency of the photovoltaic panels [2]. Due to carefully designed components, the solar panels do not require maintenance, but we must not neglect the effect of the deposited dirt during their operation. The significant problem

is that the annual electricity wastage can reach up to 17% [3,4]. The characterization of the process is not straightforward due to the many influencing factors. In the following (Table 1), we will outline the most common sources of surface contamination that can cause efficiency degradation [5–10].

Table 1. The most commonly occurring contamination from the environment of the solar system.

Flora and Fauna	Agriculture	Industry	Traffic
bird excrement	soil particles	dust	rubber
pollen	crop residues	fly ash	carbon black
leaves		carbon black	exhaust gas
		construction sites	

The effect of contaminants from the environment of the solar system (such as bird droppings) on the performance of the solar modules should not be neglected. In crystalline solar cells, spot-like deposited contaminants are even more critical because they significantly reduce the efficiency of a unit of cells in a row. The dust that covers the entire surface of the solar cell, which acts as a shielding effect, results in underperforming panels. Furthermore, these deposits can become thicker and more durable under extreme conditions if the modules are not cleaned regularly. Contaminants adhere more easily to the corners of the aluminium frames of the panels, as the cleaning effect of rain does not prevail in the said areas. Thick deposits can become a thermal insulating layer, which can cause the panels to overheat. The shadow effect and high temperature can further exacerbate microcracks. Large fractures disconnect other cells from power generation and reduce the performance and lifetime of the solar panel. Numerous studies have already shown that the particle size of the deposited powder is important for the change of efficiency [1,9,11–16]. The solar panel is usually not cleaned by rain. Heavy rains can clean the surface sufficiently, except for stubborn stains, but mild showers bring additional contaminants from the atmosphere. A wet dust layer can form a mud layer due to little precipitation, reinforcing the negative effects [1,5,11,14,17,18].

2. Materials and Methods

2.1. The Sun Simulator

The fundamental objective was to construct an artificial illumination for the measuring compilation, producing appropriate lighting conditions. However, simulating natural light is a complex and challenging task. Although there are standard requirements (IEC 60 904-9) for artificial lighting [17,19–21], our goal was to use a smart solution that is available to the general public (e.g., other educational institutions such as secondary schools). In the measurement setup, the maximal intensity E_{max} = 1245 W/m^2, the minimal intensity E_{min} = 407 W/m^2, and the inhomogeneity of illumination is ΔE = 50.73%. The median intensity is 874 W/m^2, and the modus intensity is 1000 W/m^2. The light power is 490.48 W [21,22]. The halogen reflectors at our disposal did not meet the standard criteria and need to be developed in the future. Figure 1 shows the lightning intensity distribution of the sunlight simulator.

It can be seen in Figure 1 that the value of light intensity in the corners and edges of the illuminated surface is low. However, considering the illuminated surface, it can be seen that the problem affecting a small part of the total surface and the homogeneity of the light intensity distribution are more satisfactory in other (internal) parts of the solar cell.

The average light intensity per solar panel (integrated mean value) can be calculated according to the value of the light intensity per cell and the area of one cell from the previously determined matrix elements of natural light intensity distribution [20].
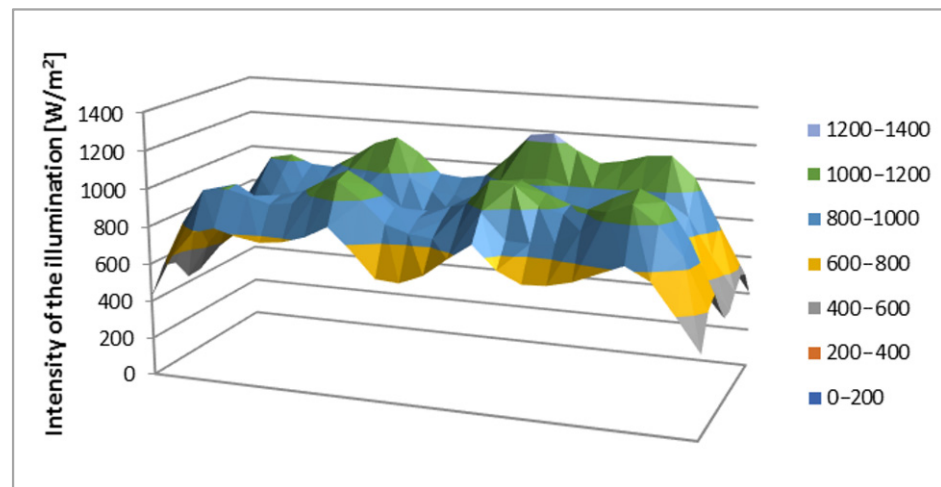
Figure 1. Reflector layout with the associated light intensity distribution.

In the measurement setup, the average intensity is $E_{average}$ = 861 W/m^2. These data correspond to a value measured on a slightly cloudy day, lower than in clear, sunny weather, which is 1000 W/m^2 in Hungary. According to Wien's law [22], a constant determination is required because there is a significant spectral energy shift between halogen reflector light and natural sunlight. Based on Figure 2, the constant of the light spectral composition is 0.532, which is the quotient of the areas under the curve and determined by a spectrophotometer [1,20,23,24]. It means that with a halogen reflector solar simulator compared to natural sunlight, the measured current is 53.2% of the real one (Figure 2).
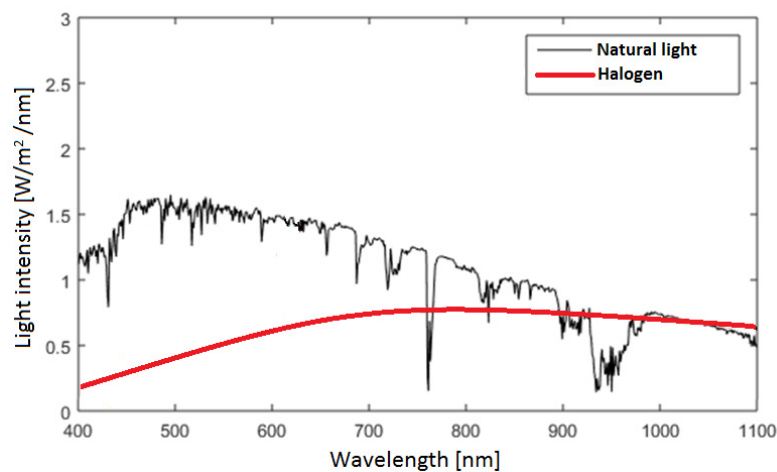
Figure 2. Difference in light intensity between natural and artificial (halogen) light.

2.2. The Measurements Composition

The monocrystalline silicon solar panel (Korax Solar, KS-80/12) was placed on a measuring table in the Renewable Energy Laboratory of our department during the research. A two-piece four-channel YC-747D digital thermometer was used to measure the surface temperature of the investigated solar panel. The eight sensors were evenly distributed on the panel surface. Figure 3 shows the measurement setup through two examples, and Table 2 shows the most important manufacturer data of the investigated solar panel. Furthermore, a METRIX MX-59HD digital multimeter was used to measure the voltage and current of the photovoltaic panel. The ambient temperature on average was 22 °C.

(a)   (b)

Figure 3. Sand-contaminated solar panel (**a**) and fly ash-contaminated solar panel (**b**).

Table 2. Parameters of the investigated solar panel specified by the manufacturer [20].

Parameter	Symbol	Value	Unit
Year of manufacture	-	2008	-
Intensity of illumination	E_{ill}	861	W/m^2
Peak Power	P_{max}	85	W
Maximum power current	I_M	4.86	A
Maximum power voltage	U_M	17.50	V
Short-circuit current	I_{SC}	5.40	A
Open-circuit voltage	U_{OC}	21.20	V
Nominal fill factor	φ	0.74	-
Serial resistance	R_s	0.0035	Ω
Parallel resistance	R_P	10,000	Ω
Number of serial-connected cells	N_S	18	piece
Number of parallel-connected cells	N_P	2	piece
Percentage Temperature coefficient for P_{max}	μ_{Pm}	−0.460	%/°C
Percentage Temperature coefficient for I_{sc}	μ_{Isc}	0.031	%/°C
Percentage Temperature coefficient for U_{oc}	μ_{Uoc}	−0.348	%/°C
Efficiency (maximal power)	η	12.75	%
Nominal operating temperature	T_N	25	°C

We wanted to demonstrate that the method of sprinkling has a measurable influencing effect on electrotechnical parameters. In previous measurements, sprinkling was usually done only with a spoon. However, in recent experiments, the sprinkling of contaminants was repeated with three tools: two sieves of different hole diameters and a plastic spoon.

It is more effective to use sieving instead of simple sprinkling. Expected consequences justifying the need for sieving:

- Pollutants can spread almost evenly over the entire surface.
- It can approximate the natural deposition much better.
- It eliminates significant particle size differences.
- A more significant reduction in performance will make it challenging to supply consumers with the solar system adequately.

Contaminant doses were measured with a Voltcraft PS-200B jewelry scale. During the experiments, the amount of contaminant was increased in increments of 5 g to 75 g. Three materials were tested: soil, sand, and ash. The soil sample comes from a functioning solar power plant and contains a large amount of clay, while the ash sample comes from a biomass power plant. The sand sample comes from an area of Hungary affected by desertification. Table 3 contains the details of the applied pollutants. Our basic assumption is that the larger Blaine specific surface contaminant will result in higher coverage, resulting in a more significant loss of solar cell production. Furthermore, the temperature increase is more significant for materials with high heat capacity and low thermal conductivity.

Fractions of different particle sizes were pre-screened so that upon application to the surface of the solar cell, all materials could fall to the surface (Table 4).

Table 3. Physical properties of dust.

Pollutant	Density [g/cm³]	Specific Surface Area [mm²/g]	Specific Heat Capacity [kJ/kgK]	Thermal Conductivity [W/mK]	Thermal Conductivity Factor [10⁻⁶ m²/s]
Soil	1.50	~0.35	0.88	0.27	0.20
Sand	1.60	~0.30	0.80	1.28	1.00
Fly ash	0.60	~0.66	1.20	0.12	0.14

Table 4. Relationship between sprinkling tools and contaminants used in the tests.

	Tool 1	Tool 2	Tool 3
Type of tool	sieve	sieve	spoon
Hole diameter	0.5 mm	0.9 mm	-
The particle size of soil, sand, and fly ash	<0.5 mm	0.5–0.9 mm	soil: 1–6 mm sand: 0.3–3 mm fly ash: 0.1–1.4 mm

3. Results

Before the investigations, a warming process eliminated the transient temperature phenomenon when electrical parameters change rapidly. After 20 min, the surface temperature of the panel increased from 23 °C to over 70 °C, and there was no measurable change in electrotechnical parameters. This transient temperature phenomenon and its effects have been reported previously [20]. Then, after the warming process, we started to spread powder on the surface.

As we want to present the decrease of measured electrotechnical parameters, we use percentage deviations. The initial value measured at the beginning of the tests (17.5 V in case of voltage, and 76.6 °C in case of average surface temperature) is also the maximum value in each measurement series, so the diagrams show the percentage deviation from this initial value. As a result, all diagrams start at the origin, so the measurement series with trend lines better illustrates the investigations' differences. Figure 4 shows the voltage drop due to the thermal insulation effect of the contaminant layer in the case of soil. It can be observed that there was a significantly larger voltage drop in the case of sieving already in the initial stage of the measurements. This can be explained by the fact that it was possible to quickly cover large parts of the surface with contaminants by sieving. There have already been publications (Abderrezek et al. [5], Bhattacharya et al. [17] and Oh et al. [25]) that differ in their methodology but show similar trends in the change of electrotechnical parameters due to surface contamination in these studies.
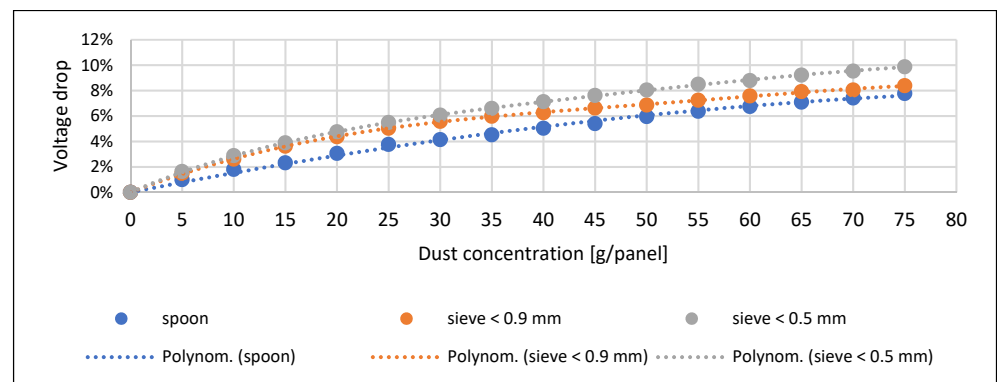
Figure 4. The open-circuit voltage values as a function of the soil concentration.

The decrease in current is affected by the degree of illumination. The more significant shading effect of the sprinkled contaminant, which spreads better on the surface of the solar panel, resulted in a significant reduction. Figure 5 shows the current-reducing effect of soil dust, and Figure 6 shows the power loss caused by soil.
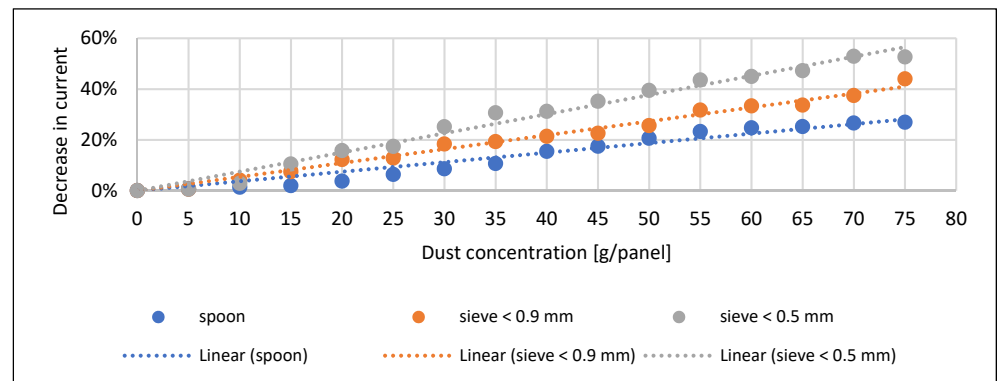
Figure 5. The short-circuit current values as a function of the soil concentration.
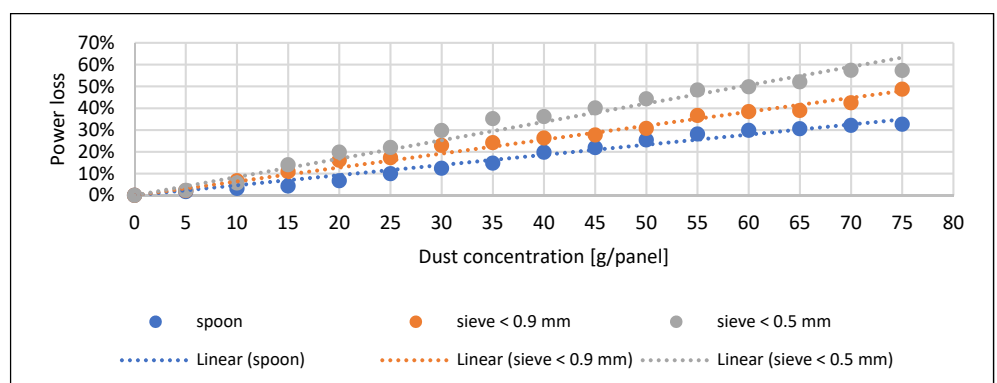
Figure 6. Power loss values as a function of the soil concentration.

In the case of sand, the maximum voltage drop was 8% (Figure 7). However, in the case of soil, this value was 10% (Figure 4). This difference can be explained by the fact that sand has a brighter surface and reflects more light. As a result, the heat absorption capacity is smaller, and the voltage values are lower than in the case of a clean panel surface. Furthermore, it was more difficult to spread the sand evenly with a spoon than in the case of soil. In the case of sand up to a 30 g/panel concentration, there was no significant difference in current reduction between the different sprinkling modes (Figure 8), as well as in the case of power loss in Figure 9. This can be explained by the fact that there is less variation between the sand particles, with fewer tiny parts than the soil. Similar trends can be observed in the study of Abderrezek et al. [5], Bhattacharya et al. [17], and Oh et al. [25].

Only at higher concentrations could significant differences be observed, which were already due to the degree of spreading on the surface. In the case of the sand, the finest particle size caused the maximum current reduction. In the case of the soil, the order and pattern of the trend lines correspond to the pre-expected picture. The voltage drop measured when the fly ash spread with a spoon is significantly lower than the results obtained with sieving. This drop can be explained by the fly ash forming a thick thermal insulating layer over the entire surface of the solar cell during sieving (Figure 10). The current decrease and power loss are smaller at higher concentrations due to the early and significant spreading material on the surface due to the density of the material (Figures 11 and 12). Similar trends can be observed in the study of Abderrezek et al. [5], Bhattacharya et al. [18], and Oh et al. [26].
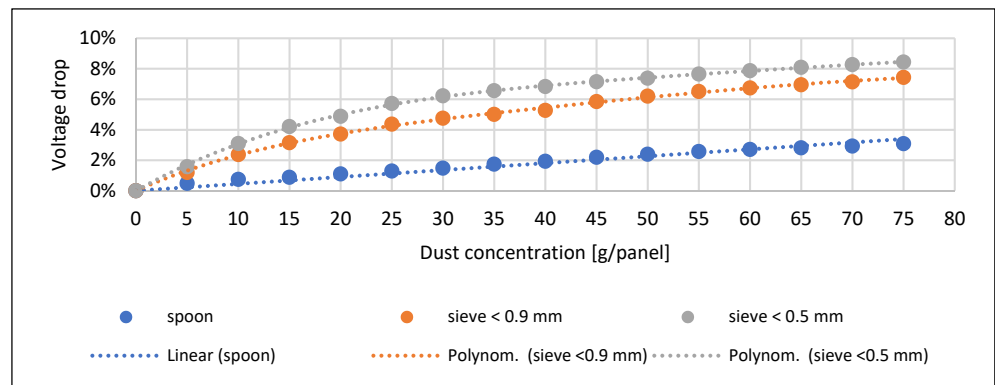
Figure 7. The open-circuit voltage values as a function of the sand concentration.
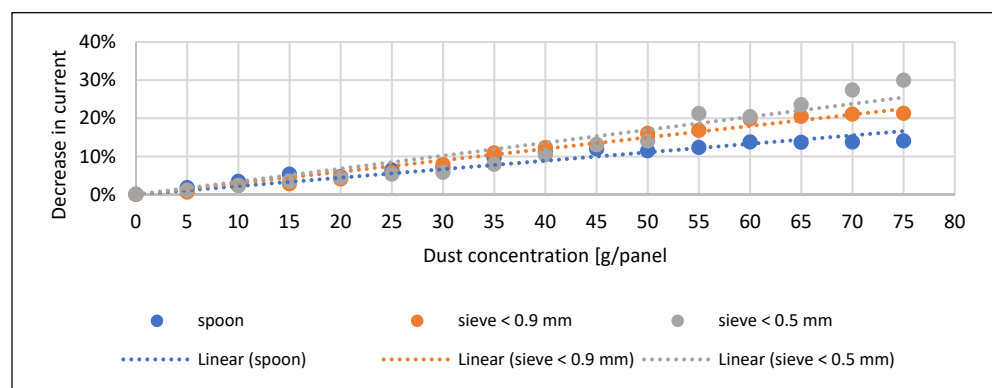
Figure 8. The short-circuit current values as a function of the sand concentration.
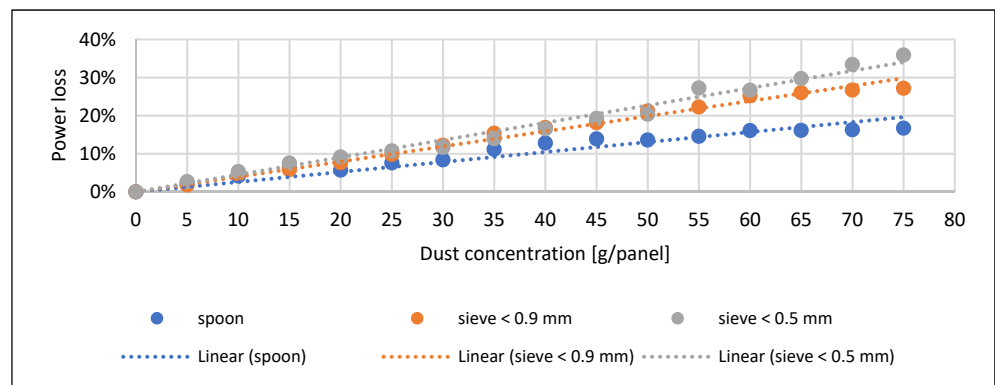
Figure 9. Power loss values as a function of the sand concentration.

As a result of the soiling, the temperature of the solar cell increased. In addition to the dust concentration, the type and size of the powder (density, heat capacity, and thermal conductivity) also influenced the temperature increase. The temperature of the solar cell contaminated with sand increased the least. Even at the highest dust concentrations, the temperature increase was only 0.5, 1.25, and 1.27 K. For soil-contaminated solar cells, these values are 1.93, 2.68, and 4.58 K. The most drastic temperature rise is by the ash: 8.73, 25.31, and 34.64 K. The difference between the thermal imaging and the contact thermometer measurement was less than 2 K (°C). The following figures illustrate the results obtained (Figures 13–15). The trend resulted in what was expected based on the mechanical and thermal properties of each material.
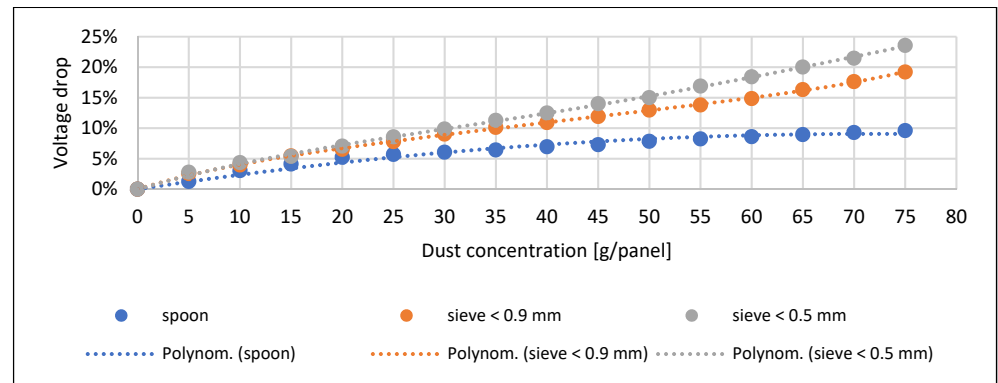
Figure 10. The open-circuit voltage values as a function of the fly ash concentration.
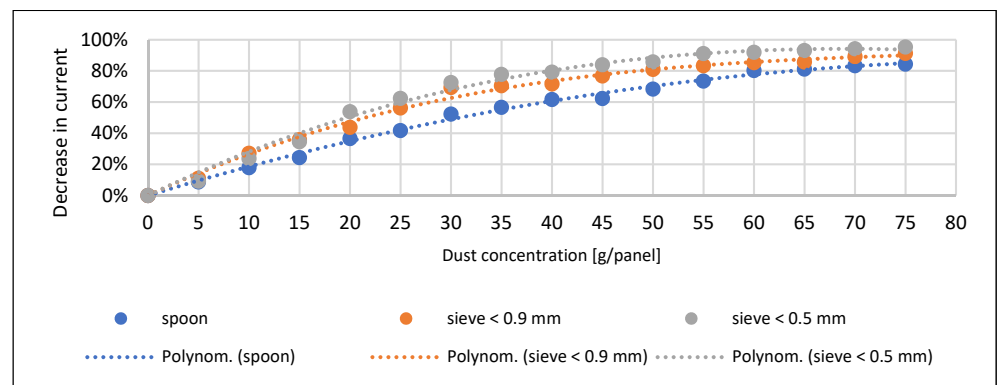
Figure 11. The short-circuit current values as a function of the fly ash concentration.
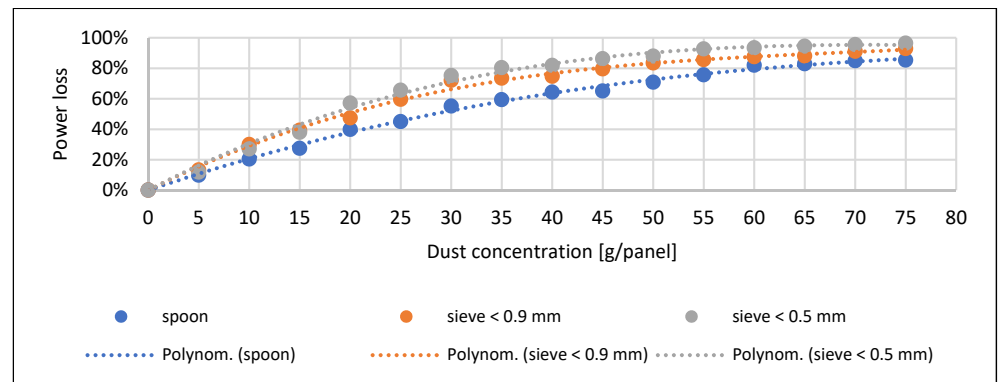
Figure 12. Power loss values as a function of the fly ash concentration.

The dust used in our measurements is common in the environment. Soil contamination is primarily heavy in the environment of agricultural cultivation and agricultural roads. Thus, large-scale, aboveground (hundreds of kW and MW) solar power plants are exposed to this pollutant.

Sand is primarily a problem in the desert environment. However, it is not uncommon to appear in Europe. The so-called "transported Saharan sand" has an even more significant effect, scratching the surface of the glass covering the solar cell due to its sharp particle structure. These changes in the surface structure usually increase the reflection. As a result, the efficiency of the solar panel decreases, but the cells are not damaged. Sandstorms are not uncommon in deserts, so there is an increased risk there.
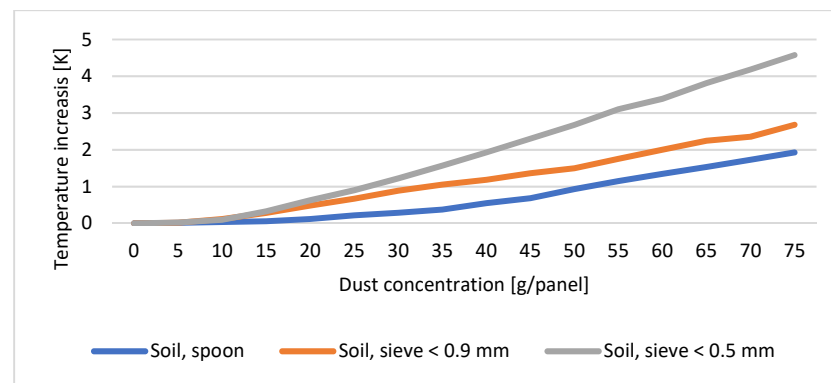
Figure 13. The temperature increase as a function of the soil concentration.
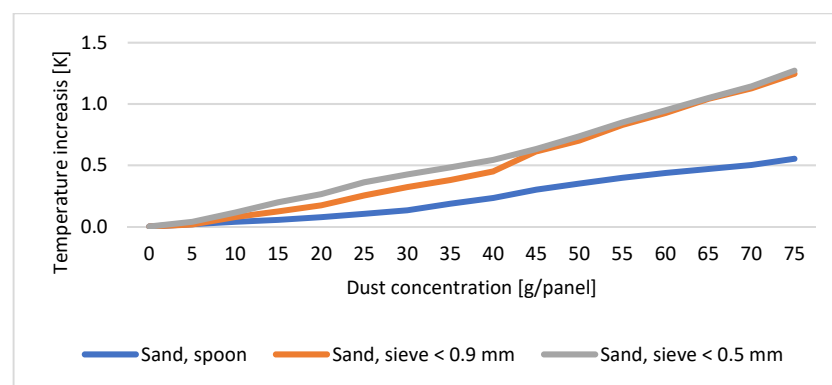
Figure 14. The temperature increase as a function of the sand concentration.
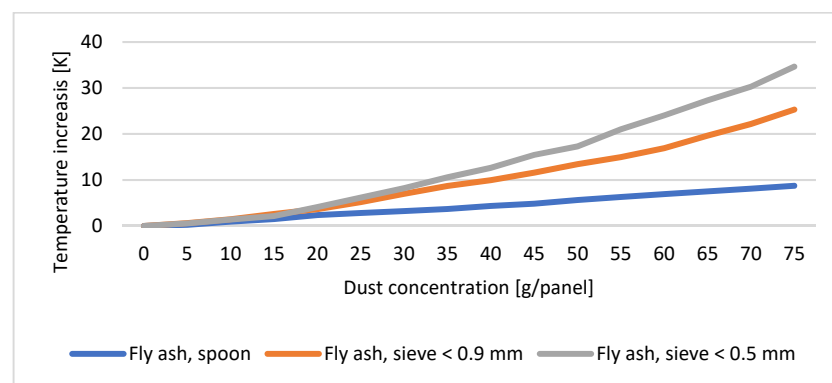
Figure 15. The temperature increase as a function of the fly ash concentration.

The fly ash can come also from residential firing and from power plants, which occurs in solar panels installed on the sloping roof (self-contained houses). We have seen that fly ash can cause a huge temperature increase, which can even cause a flammable state.

4. Discussion

Surface contaminants can cause hot spots to form, which can significantly reduce the life of the affected cells. Manufacturing defects in the cells of the solar panel, such as microcracks, can continue to grow. Thermal fluctuations can cause solar cells to fragment, leading to immediate destruction. In addition, the solder points may loosen in case of overheating the entire structure, increasing the transient contact resistance. Due to contact errors, the whole string inside the panel may fall out of production [26,27].

Our future goal is to subject the solar panels used in our measurements to an electro-luminescence test, which can visualize the damage to the solar cell. One of our industrial

partners made several electroluminescence images for us to support their work. In images taken during these investigations, properly functioning solar cells, or parts that function well, appear as bright surfaces because the photons emitted by the crystal structure are detected by the electroluminescence (EL) camera. In the dark gray parts, the crystal structure is already damaged to some extent, while the black areas show the severely damaged even ruined parts. In Figure 16, the three horizontal dark stripes showing the location of the current-collecting rails can be observed in each cell and should not emit light. Overall, several damages have occurred since its installation on the solar panel shown in Figure 16. However, the time and order of their formation cannot be determined from a single image [28–31].
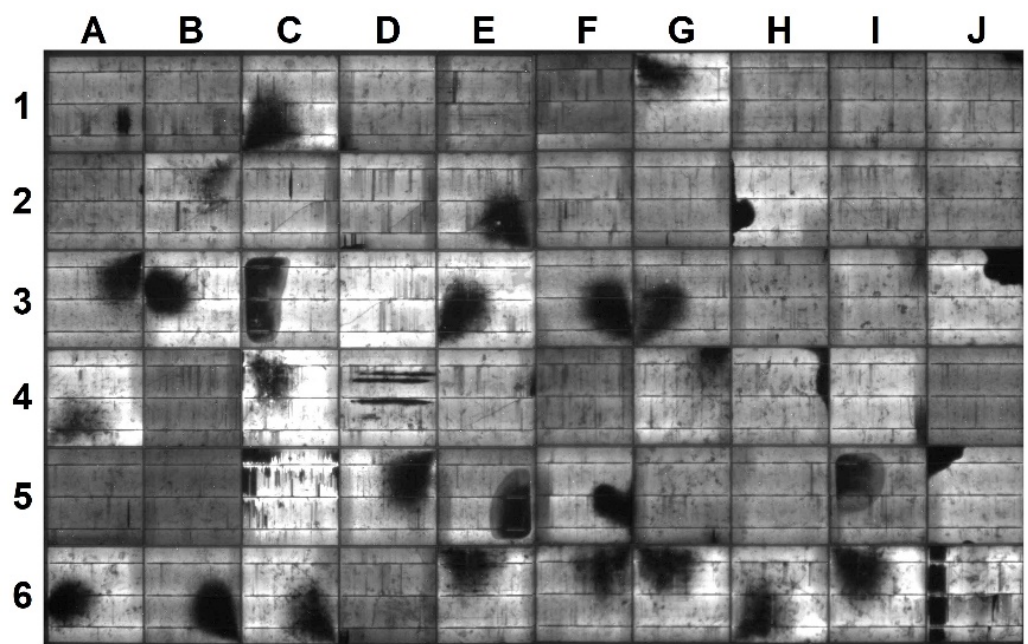
Figure 16. Electroluminescence image of a solar panel with signs of surface contamination.

The EL image of the panel shown in Figure 16 shows many cells with the sign of material defect, such cells, e.g., B3, C1, E2, and E3. In addition, several other significant injuries can be observed. A large break reduces the performance of the solar cell on cells H2, J3, and J5. These are cells from which a visibly large part has been broken, which has become inactive and does not produce electricity, so it appears completely black on the image. A unique form of damage called finger interruption can also be applied to cells B2, C2, and D2. Other significantly damaged cells are C5, D4, and J6, which show large areas of inactive parts.

This panel operated for four years at a power plant after being replaced during a review due to its insufficient electrical parameters. The air pollution in the vicinity of the solar power plant was high, causing the failure of many modules. The soil and ash samples came from this area. The original peak power of this module was 260 W, while in post-decommissioning laboratory tests, this value was only 233.8 W (89.9%). Figure 17 shows enlarged images of eight cells from the previous image (Figure 16) to make them more visible. We think surface contaminants can further exacerbate existing damage. Tang et al. [30] and Akram et al. [32] reported similarly damaged cells.
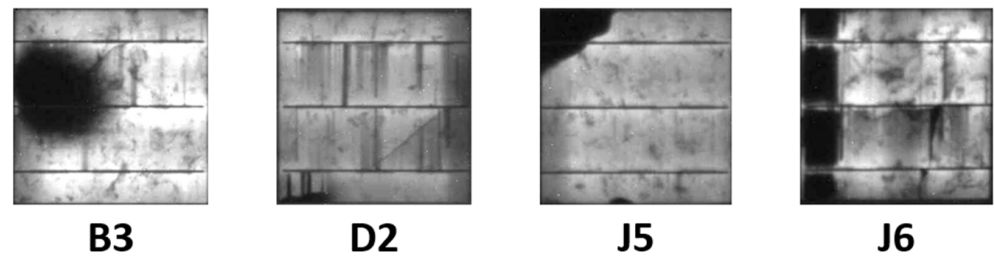
Figure 17. Examples for several solar cell defects.

Because sunlight is also a heat source, it causes a certain amount of voltage drop. Dust deposits accumulate the heat of light, thereby enhancing its negative impact. On the other hand, the shading effect of contamination can cause a decrease in current, which is further exacerbated by contamination. The decrease in power generated by the solar panel is a significant problem. It can be seen from the results that the voltage decreases due to dirt. In addition, the current output is also reduced, thus shifting the operating point. As a result, the inverter will control it differently. Solar systems can be divided into several strings on a system, which control each other independently, but the output AC voltage will be the same. Dirty or already damaged panels that produce less power reduce system performance. If the solar cell permanently operates at a higher temperature due to the surface contamination, the service life is reduced due to the negative temperature dependence of the electronics. If there are many weak panels within a string, they will be disconnected from the system.

Measurements similar to electroluminescent experiments can also be performed with a thermal capturing camera, in which case the temperature distribution can be observed. The two test methods must show a consistent pattern [31,33], as the resistance of the dark parts seen in the EL images is higher, and thus the temperature increase is higher. Studies of this nature are in progress in our laboratory. Figure 18 shows recordings of measurement of the effect of contaminants. The images were taken during the panel cooling process in a closed box. The lighting has already been switched off. The thermography diagram shows where the dust is, and it appears in much warmer areas. This temperature difference can also be measured with a contact thermometer.

(**a**)   (**b**)
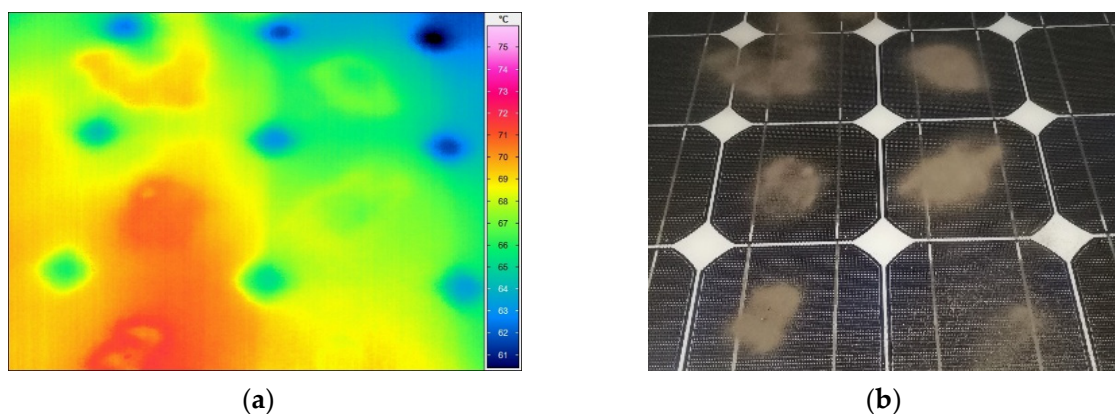
Figure 18. (**a**) Thermographic picture and (**b**) normal image of the solar panel.

5. Conclusions

Because the solar cell is exposed to light, it is also a heat source, causing a certain amount of voltage drop. Dust deposits accumulate heat, and the decrease in illumination enhances its negative impact. The decrease in the current generated by the solar panel is a significant problem due to reduced performance. It can be seen from the results that the voltage decreases due to dirt.

In summary, all measurement results are consistent with the reducing effect on electrotechnical parameters for impurities of different particle sizes. In our experience, the smaller particles caused a more significant decrease in electrotechnical parameters. The effect of fly ash powder shows a polynomial change in power as a function of dust concentration. This can be explained by the low density and the thick thermal insulation layer. The soil and sand contaminants show a close, linear power reduction.

We believe that the contaminants deposited on the surface and their degrading effects can be illustrated and demonstrated by thermal imaging and EL tests. Thermal imaging can be used not only in the laboratory, but also outdoors. Damaged solar panels can be easily searched for because their broken parts are significantly warmer than their surroundings. We are currently working on such studies, and we aim to present their results in the future.

Author Contributions: The authors contributed equally to the paper, including design, I.B.; implementation, I.B.; data gathering, D.M.-K.; modeling, I.B. and discussion of the outcomes, D.M.-K.; review and editing, I.B. and D.M.-K.; visualization, I.B. and D.M.-K. All authors have read and agreed to the published version of the manuscript.

Institutional Review Board Statement: Not applicable.

Informed Consent Statement: Not applicable.

Data Availability Statement: Not applicable.

Conflicts of Interest: The authors declare no conflict of interest.

References

1. Bodnár, I.; Iski, P.; Koós, D.; Skribanek, Á. Examination of electricity production loss of a solar panel in case of different types and concentration of dust. In *Advances and Trends in Engineering Sciences and Technologies III*, 1st ed.; Al Ali, M., Platko, M., Eds.; Taylor & Francis Group: London, UK, 2019; pp. 313–318. [CrossRef]
2. Alonso-Montesinos, J.; Martínez, F.R.; Polo, J.; Martín-Chivelet, N.; Batlles, F.J. Economic effect of dust particles on photovoltaic plant production. *Energies* **2020**, *13*, 6376. [CrossRef]
3. Ndiaye, A.; Kébe, C.M.F.; Bilal, B.O.; Charki, A.; Sambou, V.; Ndiaye, P.A. Study of the correlation between the dust density accumulated on photovoltaic module's surface and their performance characteristics degradation. *Innov. Interdiscip. Solut. Underserved Areas* **2018**, *204*, 31–42. [CrossRef]
4. Maghami, M.R.; Hizam, H.; Gomes, C.; Radiz, M.A.; Rezadad, M.I.; Hajighorbani, S. Power loss due to soiling on solar panel: A review. *Renew. Sustain. Energy Rev.* **2016**, *59*, 1307–1316. [CrossRef]
5. Abderrezek, M.; Fathi, M. Experimental study of the dust effect on photovoltaic panels' energy yield. *Sol. Energy* **2017**, *142*, 308–320. [CrossRef]
6. Gürtürk, M.; Benli, H.; Ertürk, N.K. Effects of different parameters on energy—Exergy and power conversion efficiency of PV modules. *Renew. Sustain. Energy Rev.* **2018**, *92*, 426–439. [CrossRef]
7. Said, S.A.M.; Hassan, G.; Walwil, H.M.; Al-Aqeeli, N. The effect of environmental factors and dust accumulation on photovoltaic modules and dust-accumulation mitigation strategies. *Renew. Sustain. Energy Rev.* **2018**, *82*, 743–760. [CrossRef]
8. Jiang, H.; Lu, L.; Sun, K. Experimental investigation of the impact of airborne dust deposition on the performance of solar photovoltaic (PV) modules. *Atmos. Environ.* **2011**, *45*, 4299–4304. [CrossRef]
9. Klugmann-Radziemska, E. Shading, dusting and incorrect positioning of photovoltaic modules as important factors in performance reduction. *Energies* **2020**, *13*, 1992. [CrossRef]
10. Liu, X.; Yue, S.; Lu, L.; Li, J. Study on dust deposition mechanics on solar mirrors in a solar power plant. *Energies* **2019**, *12*, 4550. [CrossRef]
11. Rao, A.; Pillai, R.; Mani, R.; Ramamurthy, M. An experimental investigation into the interplay of wind, dust and temperature on photovoltaic performance in tropical conditions. In Proceedings of the 12th International Conference on Sustainable Energy Technologies, Hong Kong, China, 26–29 August 2013; pp. 2303–2310.
12. Adinoyi, M.J.; Said, S.A.M. Effect of dust accumulation on the power outputs of solar photovoltaic modules. *Renew. Energy* **2013**, *60*, 633–636. [CrossRef]
13. Zhang, C.; Shen, C.; Yang, Q.; Wei, S.; Lv, G.; Sun, C. An investigation on the attenuation effect of air pollution on regional solar radiation. *Renew. Energy* **2020**, *161*, 570–578. [CrossRef]

14. Abass, K.I.; Al-Zubaidi, D.S.M.; Al-Waeli, A.A.K. Effect of pollution and dust on PV performance. *Int. J. Civ. Mech. Energy Sci.* **2017**, *3*, 181–185.
15. Saber, H.H.; Hajiah, A.E.; Alshehri, S.A.; Hussain, H.J. Investigating the effect of dust accumulation on the solar reflectivity of coating materials for cool roof applications. *Energies* **2021**, *14*, 445. [CrossRef]
16. Al Siyabi, I.; Al Mayasi, A.; Al Shukaili, A.; Khanna, S. Effect of soiling on solar photovoltaic performance under desert climatic conditions. *Energies* **2021**, *14*, 659. [CrossRef]
17. Bhattacharya, T.; Chakraborty, A.K.; Pal, K. Influence of environmental dust on the operating characteristics of the solar PV module in Tripura, India. *Int. J. Eng. Res.* **2015**, *4*, 141–144. [CrossRef]
18. Alghamdi, A.S.; Bahaj, A.S.; Blunden, L.S.; Wu, Y. Dust removal from solar PV modules by automated cleaning systems. *Energies* **2019**, *12*, 2923. [CrossRef]
19. Siddiqui, R.; Kumar, R.; Jha, K.G.; Morampudi, M.; Rajput, P.; Lata, S.; Agariya, S.; Nanda, G.; Raghava, S.S. Comparison of different technologies for solar PV (Photovoltaic) outdoor performance using indoor accelerated aging tests for long term reliability. *Energy* **2016**, *107*, 550–561. [CrossRef]
20. Bodnár, I. Electric parameters determination of solar panel by numeric simulations and laboratory measurements during temperature transient. *Acta Polytech. Hung.* **2018**, *15*, 59–82.
21. Hussain, F.; Othman, M.Y.H.; Yatim, B.; Ruslan, H.; Sopian, K.; Anaur, Z.; Khairuddin, S. Fabrication and irradiance mapping of a low cost solar simulator for indoor testing of solar collector. *J. Sol. Energy Eng.* **2011**, *133*, 4. [CrossRef]
22. Singh, P.; Ravindra, N.M. Temperature dependence of solar cell performance—An analysis. *Sol. Energy Mater. Sol. Cells* **2012**, *101*, 36–45. [CrossRef]
23. Bodnár, I.; Koós, D. Determination of temperature coefficient and transient electrical characteristics of a cooled and non-cooled solar module. In Proceedings of the 2018 19th International Carpathian Control Conference (ICCC), Szilvasvarad, Hungary, 28–31 May 2018; pp. 570–573. [CrossRef]
24. Kádár, P.; Varga, A. Measurement of spectral sensitivity of PV cells. In Proceedings of the 2012 IEEE 10th Jubilee International Symposium on Intelligent Systems and Informatics, Subotica, Serbia, 20–22 September 2012; pp. 549–552.
25. Oh, S.; Figgis, B.W.; Rashkeev, S. Effect of thermophoresis on dust accumulation on solar panels. *Sol. Energy* **2020**, *211*, 412–417. [CrossRef]
26. Ürmös, A.; Farkas, Z.; Dobos, L.; Nagy, S.; Nemecsics, Á. Contact problems in GaAs-based solar cells. *Acta Polytech. Hung.* **2018**, *15*, 99–124.
27. Tang, S.; Xing, Y.; Chen, L.; Song, X.; Yao, F. Review and a novel strategy for mitigating hot spot of PV panels. *Sol. Energy* **2021**, *214*, 51–61. [CrossRef]
28. Frazão, M.; Silva, J.A.; Lobato, K.; Serra, J.M. Electroluminescence of silicon solar cells using a consumer grade digital camera. *Measurement* **2017**, *99*, 7–12. [CrossRef]
29. Deitsch, S.; Christlein, V.; Berger, S.; Buerhop-Lutz, C.; Maier, A.; Gallwitz, F.; Riess, C. Automatic classification of defective photovoltaic module cells in electroluminescence images. *Sol. Energy* **2019**, *185*, 455–468. [CrossRef]
30. Tang, W.; Yang, Q.; Xiong, K.; Yan, W. Deep learning based automatic defect identification of photovoltaic module using electroluminescence images. *Sol. Energy* **2020**, *201*, 453–460. [CrossRef]
31. Olivares, D.; Ferrada, P.; Bijman, J.; Rodríguez, S.; Trigo-González, M.; Marzo, A.; Rabanal-Arabach, J.; Alonso-Montesinos, J.; Batlles, F.J.; Fuentealba, E. Determination of the soiling impact on photovoltaic modules at the coastal area of the Atacama desert. *Energies* **2020**, *13*, 3819. [CrossRef]
32. Akram, M.W.; Li, G.; Jin, Y.; Chen, X.; Zhu, C.; Zhao, X.; Khaliq, A.; Faheem, M.; Ahmad, A. CNN based automatic detection of photovoltaic cell defects in electroluminescence images. *Energy* **2019**, *189*, 116319. [CrossRef]
33. Berardone, I.; Lopez Garcia, J.; Paggi, M. Analysis of electroluminescence and infrared thermal images of monocrystalline silicon photovoltaic modules after 20 years of outdoor use in a solar vehicle. *Sol. Energy* **2018**, *173*, 478–486. [CrossRef]